01 Apr 1996

Fine-structure effect for (e,2e) collisions

Don H. Madison
Missouri University of Science and Technology, madison@mst.edu

V. D. Kravtsov

Stephenie J. Jones

Robert P. McEachran

Recommended Citation

D. H. Madison et al., "Fine-structure effect for (e,2e) collisions," *Physical Review A - Atomic, Molecular, and Optical Physics*, vol. 53, no. 4, pp. 2399-2406, American Physical Society (APS), Apr 1996.
The definitive version is available at https://doi.org/10.1103/PhysRevA.53.2399

Fine-structure effect for $(e,2e)$ collisions

D. H. Madison, V. D. Kravtsov, and S. Jones
Physics Department, University of Missouri–Rolla, Rolla, Missouri 65401

R. P. McEachran
Department of Physics and Astronomy, York University, Toronto, Ontario, Canada M3J 1P3

(Received 9 November 1995)

For the case of inelastic electron-atom scattering, it has been known for some time that significant spin effects may be observed even if spin-dependent forces on the projectile can be ignored. These spin effects result from the Pauli principle and this phenomenon has become known as the fine-structure effect. Recently, the question of whether or not these same types of effects should be observed for atomic ionization has been considered and the initial indications are that significant spin asymmetries can also be expected for atomic ionization if the final ion satisfies LS coupling and the final J state of the ion can be resolved. In this paper, we consider this problem for electron-impact ionization of inert gases. The theory of the fine-structure effect is presented for ionization and first-order distorted-wave results are compared with very recent experimental data.

PACS number(s): 34.80.Dp

I. INTRODUCTION

The field of electron-impact ionization of atoms $(e,2e)$ is now two decades old. In that period of time, significant progress has been made in several aspects of the problem and much has been learned as a result of this work. Over the years, both the experiments and theories have improved dramatically. Experiments are now able to measure absolute triple differential cross sections (TDCS) for both in-plane and out-of-plane geometries. This work has focused much interest on understanding the final-state correlations of this three-body problem where two continuum electrons emerge from a positively charged core [1].

Although there have been numerous studies of the $(e,2e)$ problem, little attention has been paid to spin effects in these collisions [2]. For the case of electron-impact excitation of heavy rare gases, it has been shown in experimental [3] and theoretical [4–7] investigations that a nonzero spin up-down asymmetry may be observed. On one hand, this may appear to be not particularly surprising since relativistic effects are known to be important for heavy atoms and relativistic effects would logically produce spin-dependent asymmetries. On the other hand, it has been shown that significant spin asymmetries may be observed even if spin-dependent forces on the projectile electron are ignored. This effect, which has become known as the fine-structure effect, is potentially observable if: (i) the final J state of the atom may be experimentally resolved; and (ii) the atom may be described by LS coupling. The question was raised of whether the mechanism that produces these asymmetries for atomic excitation will also be important in $(e,2e)$ electron-impact ionization studies of the heavier rare gases [8].

This projectile spin dependence for ionization of heavy rare-gas atoms can be understood as follows. During the ionization process, a vacancy is produced in the closed p^6 shell. Anderson, Gallagher, and Hertel [9] have shown that for a quantization axis perpendicular to the scattering plane, the cross section for exciting the $m_l=+1$ magnetic sublevel of the ionic ^2P core is not equal to that for $m_l=-1$, and the core is said to be *oriented*. The same is true for ionization so if the final states with different values of J are resolvable in some experiment, one can say that it is equivalent in some sense to having a target of partially oriented atoms. For simplicity, let us assume that a spin-polarized electron ionizes an inert gas leaving the ion in the $^2P_{1/2}$ state. Further, assume that this state is *completely* oriented with $m_l=+1$. This situation is schematically represented in Fig. 1. For this case, the spin of the ion must be down, and as a result only a spin-up electron can be ejected. If the projectile electron also has spin up, then these two electrons are indistinguishable and there is interference between direct and exchange processes. On the other hand, if the incident electron has spin down, the electrons are distinguishable so there is no interference. As a result, the cross sections for spin up and spin down will be different. Clearly the relative size of the exchange process as well as the amount of orientation of the core play a key role in the *size* of this spin effect.

The purpose of the present paper is to investigate the spin

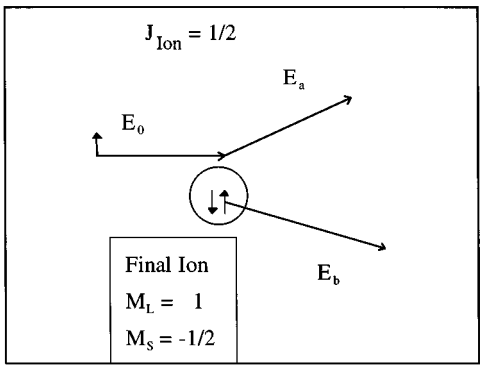

FIG. 1. Schematic representation of ionization of an inert gas by an electron with spin-up leaving the ion in a final state of $J=1/2$ and $M_L=1$. The axis of quantization is perpendicular to the scattering plane. The energy of the incident electron is E_0 while E_a and E_b are the energies of the two final-state electrons.

asymmetries that may be expected as a result of the fine-structure effect for electron-impact ionization of xenon. The theoretical model we use is the first-order distorted-wave Born (DWB1) approximation in which the final-state electron-electron correlation is approximated using effective charges. This model was proposed by Jones and co-workers [10,11] and it has previously been applied to electron-hydrogen and electron-helium ionization. Here the model is applied to ionization of the inert gases. In the spirit of the fine-structure effect, nonrelativistic wave functions are used for the projectile electron and the atom is assumed to satisfy LS coupling. For the treatment of the atom, both relativistic and nonrelativistic atomic wave functions are considered.

The paper is organized as follows. Section II contains a description of our theoretical approach. In Sec. III, the present results are compared with experiment for both unpolarized electron beams and very recent spin-polarized measurements and Sec. IV contains the conclusions. Preliminary discussion of this work may be found in Refs. [12] and [13].

II. THEORY

A. General case

Consider the ionization of an atom in an initial state with total angular momentum and projection $J_A M_A$ by an electron with spin projection μ_i. The final state will consist of two free electrons with spin projections μ_a, μ_b and an ion with total angular momentum and projection $J_f M_f$. If we ignore capture, the T matrix for this process can be expressed as

$$T^{M_A M_f}_{\mu_i \mu_a \mu_b} = F^{M_A M_f}_{\mu_i \mu_a \mu_b} - G^{M_A M_f}_{\mu_i \mu_a \mu_b}, \tag{1}$$

where F and G are the direct and exchange amplitudes, respectively. The calculations reported here were carried out using a refined version [10] of the distorted-wave Born approximation (DWBA) model of Jones, Madison, and Srivastava [11]. In this model the capture amplitude is zero. Nevertheless, the effects of capture are indirectly included, since the model includes electron exchange in the potentials and such a model *implicitly* includes the effect of capture [14]. Our experience has been that capture is only important in near-threshold $(e,2e)$ reactions. The direct amplitude is given by

$$F^{M_A M_f}_{\mu_i \mu_a \mu_b} = \sqrt{N} \langle \chi_a^-(0) \chi_b^-(1) \psi_{J_f M_f}(2 \cdots N) | V_{01} | \times \psi_{J_a M_a}(1 \cdots N) \chi_i^+(0) \rangle. \tag{2}$$

Here N is the number of electrons in the atom, $\psi_{J_A M_A}$ is the quantum mechanical wave function for the initial state of the atom, $\psi_{J_f M_f}$ is the wave function for the final state of the ion, χ_i is the wave function for the incident projectile, and χ_a, χ_b are the wave functions for the two continuum electrons. The nonrelativistic interaction potential V_{01} is given by

$$V_{01} = \frac{1}{r_{01}}, \tag{3}$$

where r_{01} is the distance between particles 0 and 1. The distorted wave χ_i^+ for the incident electron is a solution of

$$\left(-\frac{1}{2}\nabla^2 + U_{\text{atom}} \right) \chi_i^+ = E_i \chi_i^+ , \tag{4}$$

where U_{atom} is the static interaction of the incoming electron with the ground state of the atom. It is important to note that since we use a nonrelativistic Hamiltonian, U_{atom} contains no spin-dependent forces. As a result, exchange is the only process in this approach that can change the spin. The final-state distorted waves χ_a^- and χ_b^- are obtained using final-state ionic potentials U_a and U_b, respectively. Although these potentials, in principle, can be different, we have found (see Ref. [11]) that a symmetric treatment with $U_a = U_b = U_f$ is best:

$$\left(-\frac{1}{2}\nabla^2 + U_f \right) \chi_a^- = E_a \chi_a^- , \tag{5}$$

$$\left(-\frac{1}{2}\nabla^2 + U_f \right) \chi_b^- = E_b \chi_b^- , \tag{6}$$

with

$$U_f = z U_{\text{ion}} + (1-z) U_{\text{atom}} . \tag{7}$$

Here U_{ion} is the static-exchange potential for the ion and z is an effective charge that depends on the angle of observation θ_{ab} between the two final-state electrons,

$$z = 1 - \frac{1}{2\sin(\theta_{ab}/2)} . \tag{8}$$

The distorted waves obtained from Eqs. (4)–(6) are then orthogonalized to the bound-state orbital of the active electron using a Gramm-Schmidt algorithm. This orthogonalization causes the matrix elements involving single-particle operators (e.g., nuclear interactions, static distorting potentials) to vanish. If we define

$$\beta^{M_A M_f}(1) \equiv \sqrt{N} \langle \psi_{J_f M_f}(2 \cdots N) | \psi_{J_A M_A}(1 \cdots N) \rangle \tag{9}$$

the direct amplitude 2 can be written as

$$F^{M_A M_f}_{\mu_i \mu_a \mu_b} = \langle \chi_a^-(0) \chi_b^-(1) | V_{01} | \beta^{M_A M_f}(1) \chi_i^+(0) \rangle. \tag{10}$$

Likewise the exchange amplitude may be written as

$$G^{M_A M_f}_{\mu_i \mu_a \mu_b} = \langle \chi_a^-(1) \chi_b^-(0) | P_{01} V_{01} P_{01}^{-1} | \beta(1) \chi_i^+(0) \rangle, \tag{11}$$

where P_{01} is the operator that interchanges particles 0 and 1. The β factor of Eq. (9) depends on the initial and final atomic states. Here we assume that the ground state of the atom as well as the final ionic state can be represented in the LS coupling scheme (fine-structure approximation). Consequently,

$$\psi_{J_A M_A} = \sum_{M_L M_S} C(LSJ_A; M_L, M_S, M_A) | LM_L, SM_S \rangle, \tag{12}$$

where $|LM_L, SM_S\rangle$ is the properly antisymmetrized LS coupled atomic wave function and $C(l_1, l_2, l_3, m_1, m_2, m_3)$ is a Clebsch-Gordon coefficient. This wave function can be ex-

pressed in terms of single-particle wave functions by making the fractional parentage expansion [15]

$$|LM_L,SM_S\rangle=\sum_{\alpha_P S_P L_P \alpha_n l_n}\langle\alpha_P S_P L_P,\alpha_n l_n|\}\alpha LS\rangle|(\alpha_P L_P S_P,\alpha_n l_n);LM_L,SM_S\rangle. \tag{13}$$

The coefficient of fractional parentage is $\langle\alpha_P S_P L_P,\alpha_n l_n|\}\alpha LS\rangle$; L_P and S_P are the total orbital and spin angular momentum of the parent; l_n is the orbital angular momentum of the single-particle wave function; α_P, α_n, and α are any additional quantum numbers necessary to describe the particular states completely; the single-particle wave function spin quantum number, which is omitted in the coefficient of fractional parentage for the LS coupled atomic state is understood to be 1/2; and

$$|(\alpha_P L_P S_P,\alpha_n l_n);LM_L,SM_S\rangle=\sum_{M_P m_n M_{S_P}\mu_n} C(L_P l_n L;M_P,m_n,M_L)C(S_P s_n S;M_{S_P},\mu_n,M_S)|\alpha_P L_P M_P;S_P M_{S_P}\rangle \times|\alpha_n l_n m_n;s_n\mu_n\rangle. \tag{14}$$

The quantity $|\alpha_P L_P M_P,S_P M_{S_P}\rangle$ represents the antisymmetrized wave function of the $(N-1)$ particle parent state, and $|\alpha_n l_n m_n,s_n\mu_n\rangle$ is the n*th* single-particle wave function. The LS coupled final state for the ion may be expressed as

$$\psi_{J_f M_f}=\sum_{M_c M_{S_c}} C(L_c S_c J_f;M_c M_{S_c} M_f)|\alpha_c L_c M_c;S_c M_{S_c}\rangle, \tag{15}$$

where $|\alpha_c L_c M_c;S_c M_{S_c}\rangle$ is the antisymmetrized wave function for the final state of the ionic core with orbital angular momentum L_C and spin S_C. If we assume that the collision time is shorter than the relaxation time for the atom, this wave function will be one of the parent states for the initial atomic state (12). Using the expressions (13) and (15), it can be shown that β reduces to

$$\beta^{M_A M_f}(1)=\sum_{m_n\mu_n} A(M_A,M_f,m_n,\mu_n)|\alpha_n l_n m_n,S_n,\mu_n(1)\rangle, \tag{16}$$

where

$$A(M_A,M_f,m_n,\mu_n)=\sqrt{N}\sum_{M_c M_{S_c} M M_S} C(L_c S_c J_f;M_c M_{S_c} M_f)C(LSJ_A;MM_S M_A)C(L_c l_n L;M_c m_n M) \times C(S_c S_n S;M_{S_c}\mu_n M_S)\langle\alpha_c S_c L_c,\alpha_n l_n|\}\alpha LS\rangle. \tag{17}$$

Consequently, the direct amplitude (2) can be expressed as

$$F^{M_A M_f}_{\mu_i\mu_a\mu_b}=\sum_{m_n\mu_n} A(M_A,M_f,m_n,\mu_n)f_{m_n}\delta_{\mu_a\mu_i}\delta_{\mu_b\mu_n}. \tag{18}$$

The amplitude f_{m_n} is a direct scattering amplitude that depends on the orbital angular momentum projection m_n of the atomic electron that is ejected,

$$f_{m_n}=\langle\chi_a^-(0)\chi_b^-(1)|V_{01}|\alpha_n l_n m_n(1)\chi_i^+(0)\rangle. \tag{19}$$

In a similar manner, the exchange amplitude can be expressed as

$$G^{M_A M_f}_{\mu_i\mu_a\mu_b}=\sum_{m_n\mu_n} A(M_A,M_f,m_n,\mu_n)g_{m_n}\delta_{\mu_a\mu_n}\delta_{\mu_b\mu_i}, \tag{20}$$

where

$$g_{m_n}=\langle\chi_a^-(1)\chi_b^-(0)|P_{01}V_{01}P_{01}^{-1}|\alpha_n l_n m_n(1)\chi_i^+(0)\rangle. \tag{21}$$

For the case of polarized electrons incident upon unpolarized targets with no final-state spin polarization distinction, the differential cross section (DCS) is given by

$$\sigma_{J_f}(\mu_i)=\frac{(2\pi)^4}{E_i}\frac{1}{2J_A+1}\sum_{M_A M_f\mu_a\mu_b}|T^{M_A M_f}_{\mu_i\mu_a\mu_b}|^2, \tag{22}$$

where the flux factor is for continuum waves normalized to a δ function in energy.

B. Ionization of inert gases

In the present paper, we are interested in the ionization of an electron from the outer p shell of an inert gas. For this case, the fractional parentage coefficient for the parent corresponding to the residual ionic core is

$$\langle\alpha_c S_c L_c;\alpha_n l_n|\}\alpha LS\rangle=\langle\alpha_c(1/2)1;\alpha_n 1|\}\alpha 00\rangle=\sqrt{6/N} \tag{23}$$

and

$$A(0,M_f,m_n,\mu_n)=(-1)^{3/2+m_n+\mu_n} \times C[1(1/2)J_f;-m_n,-\mu_n,M_f]. \tag{24}$$

So far all our results are independent of the choice of coordinate system. To obtain explicit expressions for DCS, we need to specify the reference frame. For an inert gas, the final-state ion can have $J_f=1/2$ or 3/2. If (24) is used in (18) and (20), it can be seen that in the natural frame (Z axis perpendicular to the scattering plane) the cross sections for spin-up ($\uparrow$) or spin-down ($\downarrow$) incident electrons are given by

$$\sigma_{1/2}(\uparrow)=\frac{(2\pi)^4}{E_i}\frac{2}{3}(|f_{+1}|^2+|g_{+1}|^2+|f_{-1}-g_{-1}|^2), \tag{25}$$

$$\sigma_{1/2}(\downarrow)=\frac{(2\pi)^4}{E_i}\frac{2}{3}(|f_{-1}|^2+|g_{-1}|^2+|f_{+1}-g_{+1}|^2), \tag{26}$$

$$\sigma_{3/2}(\uparrow)=\frac{(2\pi)^4}{E_i}\left(|f_{-1}|^2+|g_{-1}|^2+\frac{1}{3}|f_{-1}-g_{-1}|^2+\frac{1}{3}|f_{+1}|^2 +\frac{1}{3}|g_{+1}|^2+|f_{+1}-g_{+1}|^2\right), \tag{27}$$

$$\sigma_{3/2}(\downarrow)=\frac{(2\pi)^4}{E_i}\left(|f_{+1}|^2+|g_{+1}|^2+\frac{1}{3}|f_{+1}-g_{+1}|^2+\frac{1}{3}|f_{-1}|^2 +\frac{1}{3}|g_{-1}|^2+|f_{-1}-g_{-1}|^2\right). \tag{28}$$

It is important to note that the m_n subscript here refers to the orbital angular momentum projection for the active electron that is removed from the atom. The corresponding projection for the residual ionic core, M_c, is simply the negative of this value since the sum of the two must be zero.

In terms of these cross sections, the spin up-down asymmetry, A_{J_f}, is given by

$$A_{J_f}=\frac{\sigma_{J_f}(\uparrow)-\sigma_{J_f}(\downarrow)}{\sigma_{J_f}(\uparrow)+\sigma_{J_f}(\downarrow)}. \tag{29}$$

For practical purposes it is useful also to obtain the expression for spin up-down asymmetry in the collision frame where the quantization axis is parallel to the momentum of the incident electron. Bartschat and Madison [6] showed that the asymmetry function in the collision frame may be written as

$$A_{J_f}=\frac{(2\pi)^4}{E_i}\frac{1}{\sigma_u}\frac{1}{2J_A+1} \times\sum_{M_A M_f \mu_a \mu_b}\mathrm{Im}\{T^{M_A M_f}_{\mu_i=1/2,\mu_a\mu_b}T^{M_A M_f *}_{\mu_i=-1/2,\mu_a\mu_b}\}, \tag{30}$$

where σ_u is the DCS for unpolarized incident particles, which can be expressed in terms of DCS from (22):

$$\sigma_u=\sum_{\mu_i}\sigma_{J_f}(\mu_i). \tag{31}$$

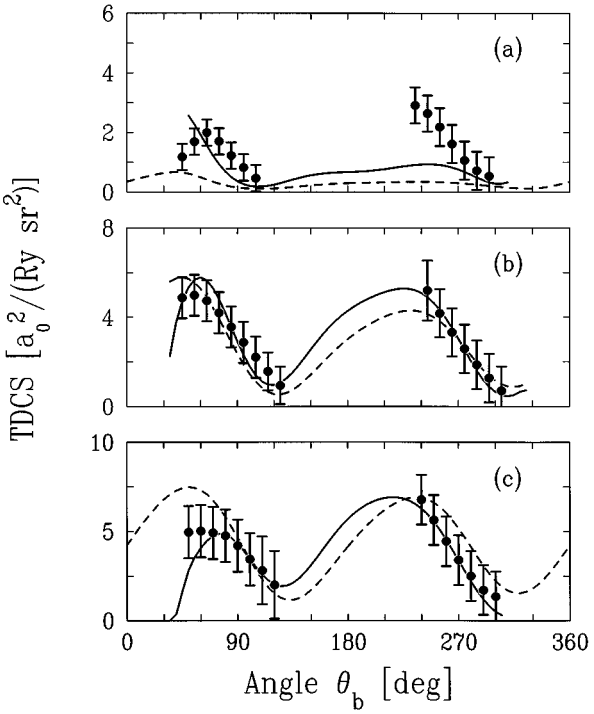

FIG. 2. TDCS for 100-eV ionization of argon. The faster final-state electron is scattered through an angle of 5° in the scattering plane. The horizontal axis of the figure indicates the angle of observation for the slower final-state electron measured clockwise from the beam direction. The coordinate system is chosen such that the faster final-state electron is scattered to the left in the scattering plane when viewed from the top. The theoretical curves are as follows: dashed curve, DWB1 and solid curve, DWB1C. The experimental data are those of [20] normalized to obtain the best overall agreement with theory. The different parts of the figure correspond to different energies for the ejected electron: (a) 20 eV; (b) 10 eV; (c) 5 eV. DWB1 results were multiplied by the factor of (a) 0.85; (b) 0.80; (c) 0.44.

Substituting Eqs. (18) and (20) into Eqs. (30) and (31) and taking into account the fact that for the collision frame $f^c_{-1}(g^c_{-1})=-f^c_1(-g^c_1)$ (the superscript c is used to distinguish the collision frame from the natural frame), we obtain, e.g., for $J_f=1/2$:

$$A_{1/2}=\frac{\sqrt{2}\,\mathrm{Im}\{f^c_1 g^{c*}_0-g^c_0 f^{c*}_1+g^c_1 f^{c*}_0-f^c_0 g^{c*}_1\}}{|f^c_0|^2+|g^c_0|^2+|f^c_0-g^c_0|^2+2|f^c_1|^2+2|g^c_1|^2+2|f^c_1-g^c_1|^2}. \tag{32}$$

One may check that Eq. (32) is equivalent to Eq. (29) by using the transformation from the natural frame amplitudes $f_{\pm1}(g_{\pm1})$ to the collision frame amplitudes $f^c_{1,0}(g^c_{1,0})$ [9]:

$$f_{\pm1}=\mp\frac{1}{\sqrt{2}}f^c_0+if^c_1. \tag{33}$$

Substituting Eq. (33) into Eqs. (25)–(29) we obtain Eq. (32).

In the present approach, the J_f dependence in the T matrix results primarily from using different atomic wave functions and excitation energies for the two different final states. It is instructive to obtain relations ignoring all fine-structure

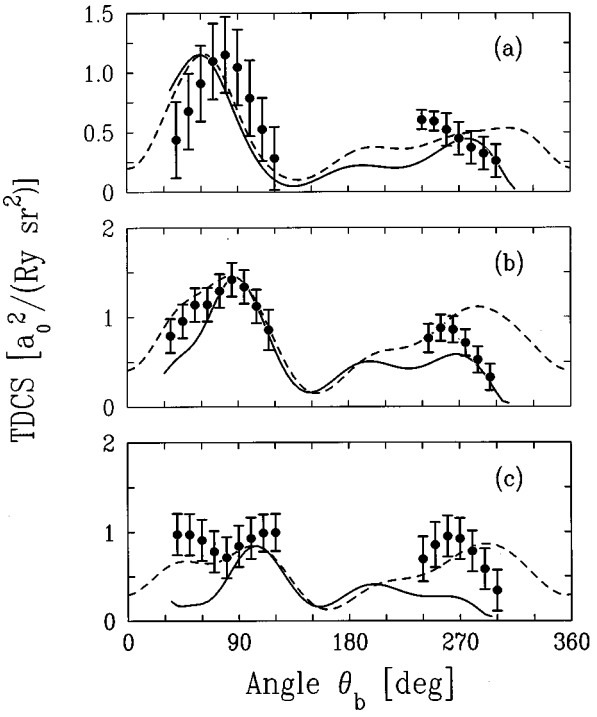

FIG. 3. The same as Fig. 2 except that the faster final-state electron is scattered through an angle of 15°. DWB1 results were multiplied by the factor of (a) 2.25; (b) 0.85; (c) 0.37.

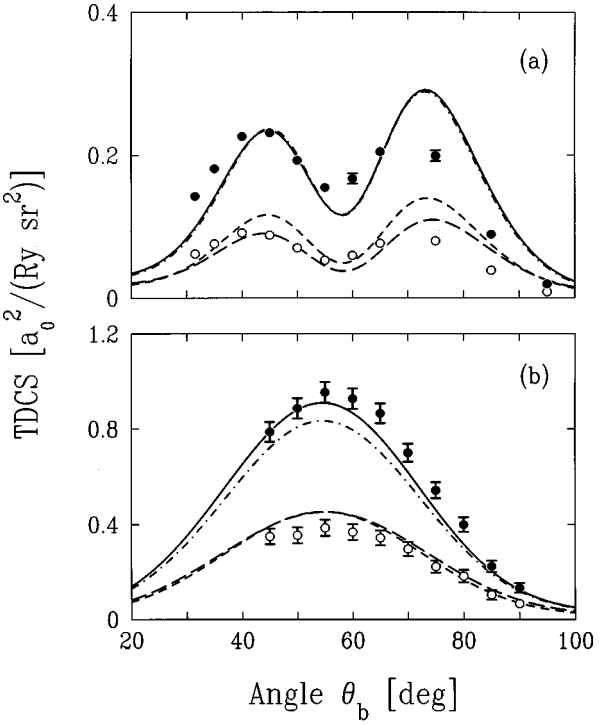

FIG. 4. Triple differential cross sections for ionization of xenon by 147-eV unpolarized electrons. The faster final-state electron has an energy of 100 eV and (a) corresponds to observing this electron at an angle of 28° and (b) corresponds to 15°. The angle θ_b corresponds to the observation angle for the slower electron measured clockwise relative to the beam direction. The experimental data are those of [20] normalized to obtain the best overall agreement with theory. The theoretical curves are as follows: solid, DWB1CR for $J_f=3/2$; dashed-dotted, DWB1C for $J_f=3/2$; long-dashed, DWB1CR for $J_f=1/2$; and short-dashed, DWB1C for $J_f=1/2$.

effects, i.e., using the same wave functions for both final states and also using the same ionization energy whether $J_f=1/2$ or 3/2. If this is done, then the direct and exchange amplitudes are independent of J_f and some useful relationships can be derived. For instance, summing the cross sections over spin (and dividing by two) gives the cross sections for unpolarized electrons, $\sigma_{1/2}$ and $\sigma_{3/2}$, which are related simply by

$$\sigma_{3/2}=2\sigma_{1/2}. \tag{34}$$

Then, the total cross section may be obtained by adding these two cross sections:

$$\sigma_{\text{total}}=\sigma_{1/2}+\sigma_{3/2}. \tag{35}$$

Furthermore, a particularly simple relationship exists between the asymmetries for $J_f=1/2$ or 3/2:

$$A_{1/2}=-2A_{3/2}, \tag{36}$$

which can be obtained by using Eqs. (25)–(28) in Eq. (29).

III. RESULTS

A. Differential cross sections

There have been limited experimental measurements of the TDCS for electron-impact ionization of the inert gases and all reported measurements to date are relative. To get a better feeling for the value of experiments using spin-polarized electrons, it is instructive to examine how well the theory predicts the TDCS for both unpolarized and polarized electrons. One of the strengths of a distorted-wave calculation is that the importance of different types of physical effects can be readily examined. In this section, we would like to concentrate on two such effects—namely, the importance of final-state correlations and the type of bound-state wave functions that should be used to describe the atom and ion. We will first consider final-state correlation. It is known that the final-state interaction between the two outgoing electrons is potentially very important and in the last section a method for including this interaction using effective charges was described. In this approach, the effective charges and consequently the distorting potentials for the two final-state electrons depend upon the angular separation of the two electrons. In the standard distorted-wave approach, on the other hand, this interaction is not included in the description of the final-state wave functions and the distorting potentials depend only on the final state of the ion. The standard distorted-wave approach (DWB1) may be obtained from the present formulation by setting $z=1$ in Eq. (7). As a result, the importance of the final-state correlations within this model may be examined by comparing DWB1 results with those obtained using the angle-dependent distorting potentials that we label DWB1C. In Figs. 2 and 3, DWB1 and DWB1C results are compared with the TDCS measurements of Ehrhardt *et al.* [16] for ionization of argon by unpolarized electrons. The experimental data were normalized to give the best overall agreement with the DWB1 results. Since the magnitude of the DWB1 and DWB1C results were significantly different, the DWB1 was normalized to the DWB1C

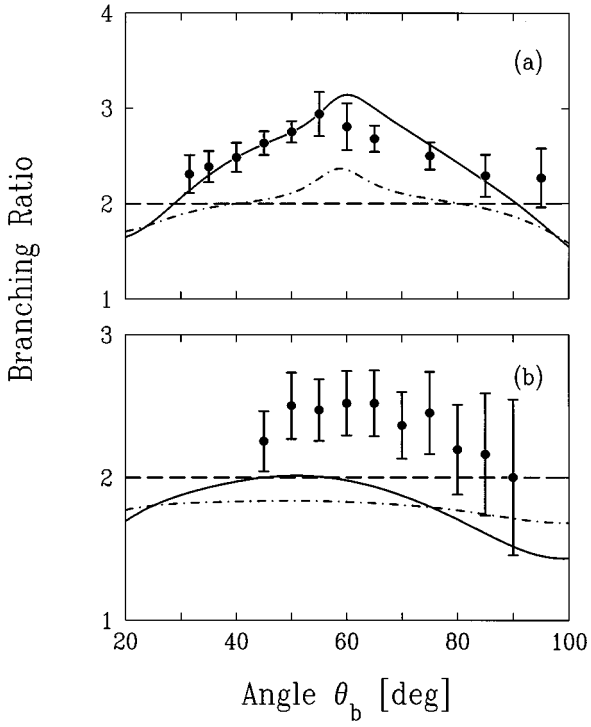

FIG. 5. Branching ratio for ionization of xenon by 147-eV unpolarized electrons. The faster final-state electron has an energy of 100 eV and (a) corresponds to observing this electron at an angle of 28° and (b) corresponds to 15°. The angle θ_b corresponds to the observation angle for the slower electron measured clockwise relative to the beam direction. The experimental data are those of [11]. The theoretical curves are as follows: solid curve, DWB1CR and dashed-dotted, DWB1C.

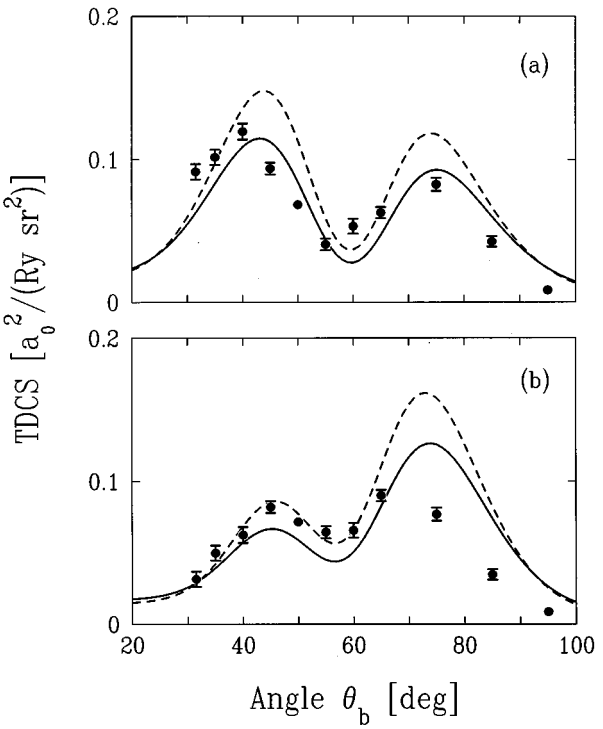

FIG. 6. Spin-dependent differential cross sections for ionization of xenon by 147-eV incident electrons. The 100-eV faster final-state electron is observed at an angle of 28° with the final-state ion being left in the $J_f = 1/2$ state. (a) corresponds to ionization by spin-up electrons and (b) corresponds to ionization by spin-down electrons. The experimental data are those of [11] normalized to obtain the best overall agreement with theory. The theoretical curves are as follows: solid curve, DWB1CR; dashed, DWB1C.

to provide a comparison between the shape of the two theories and experiment. Coefficients of normalization for the DWB1 are given in the captions. The present approximation for including correlation should be most accurate when the two electrons leave the collision at 180° apart and this approximation become less accurate as the angle between the two electrons decreases. In fact, Jones, Madison, and Hanne [12] suggested that the model should not be used for angular separations less than about 50°. Consequently, the DWB1C results are not shown for small angular separations between the two final-state electrons. From Figs. 2 and 3, it is seen that overall the shape of the DWB1C results are closer to the shape of the experimental data.

The next issue we would like to examine is the bound-state wave functions used to describe the atom and ion. The simplest approximation for these wave functions would be to use single configuration nonrelativistic Hartree-Fock. In this approximation, the outermost p orbitals are the same for both the $J_f = 1/2$ and 3/2 states. This was the approximation that was used for the argon results presented in Figs. 2 and 3. However, for the heavier atoms, the different J levels become more distinct and the procedure of using the same p orbital for both states becomes more questionable. To investigate this issue, we have performed calculations for xenon using two different sets of wave functions. For the first set, we obtained single configuration nonrelativistic Hartree-Fock wave functions for the ground state using the computer code of Froese-Fischer [17]. We then approximated the active electron wave function for both the $J_f = 1/2$ and 3/2 states by the outermost p orbital obtained from this calculation. For the second set, we obtained relativistic wave functions using the multiconfiguration Dirac-Fock code of Grant *et al.* [18], which produces both $5p_{1/2}$ and $5p_{3/2}$ orbitals for the ground state. For the case of $J_f = 1/2$ (3/2), the six electrons in the outermost shell were treated as a p orbital and a p hole and both the hole and orbital were assumed to have a J of 1/2 (3/2). The corresponding J-dependent p orbitals from Grant's code were then used for the active electron. These relativistic wave functions, of course, have large and small components whereas the rest of the theory is nonrelativistic. To use the relativistic wave functions, we dropped the small component and renormalized the large component to unity. For xenon, the large component represented 99.99% of total wave function prior to renormalization.

Nonrelativistic TDCS DWB1C results are compared with relativistic DWB1CR results for ionization of xenon by unpolarized electrons in Fig. 4. The figure contains results for the final-state ion being left in both the $J_f = 1/2$ and 3/2 states and for two different fixed angles of observation for the faster final-state electron. The experimental data are those of [19]. These are relative measurements that have been normalized to achieve the best overall agreement with theory. Since the experiment is designed to measure the ratio of TDCS for different J values, the same normalization factor is used for all four curves at each angle of observation. Interestingly, results obtained with the nonrelativistic and relativ-

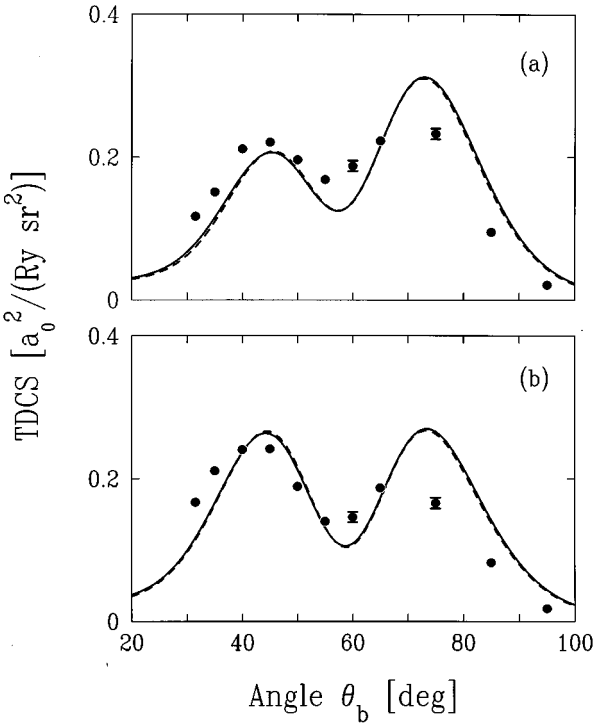

FIG. 7. Same as Fig. 6 except that $J_f = 3/2$.

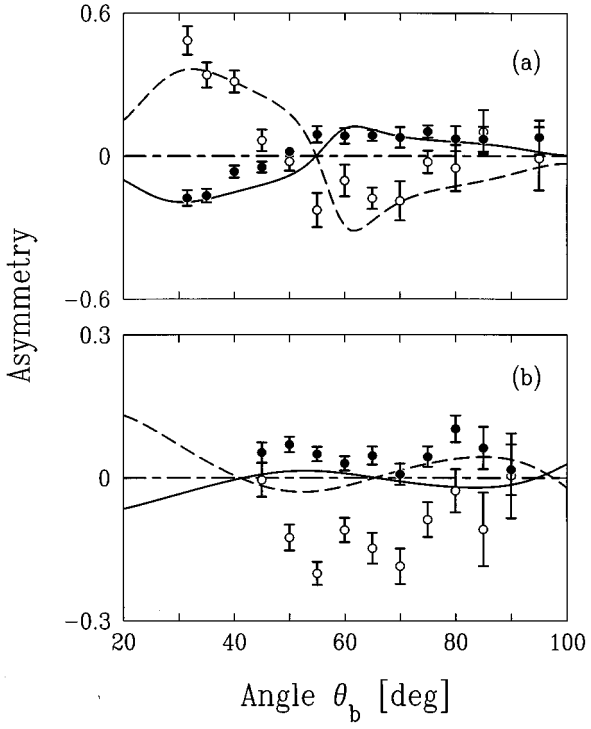

FIG. 8. Spin up-down asymmetry for 147-eV spin-polarized electron-impact ionization of xenon. The faster final-state electron has an energy of 100 eV and (a) corresponds to observing this electron at an angle of 28° and (b) corresponds to 15°. The angle θ_b corresponds to the observation angle for the slower electron measured clockwise relative to the beam direction. The experimental data are those of [11] and the solid circles correspond to $J_f = 3/2$ and the open circles correspond to $J_f = 1/2$. The theoretical curves are as follows: solid, DWB1CR for $J_f = 3/2$; dashed, DWB1CR for $J_f = 1/2$.

istic wave functions are almost identical in some cases and different in others. When there is a difference, the results with the relativistic wave functions are closer to the experimental data.

The branching ratio is defined to be the ratio of $\sigma_{3/2}/\sigma_{1/2}$. In the limit of degenerate states and the same p orbitals being used for both states, Eq. (34) may be used and the branching ratio is two. The branching ratio resulting from the nonrelativistic and relativistic wave functions are displayed in Fig. 5. It should be noted that the branching ratio is independent of normalization and the figure represents a direct comparison between experiment and theory. For the case of the nonrelativistic DWB1C calculation (dashed-dotted), the deviation from two results from using the proper ionization energies (13.44 and 12.13 eV, respectively, for $J_f = 1/2$ or 3/2) in the calculation of the wave function for the two final-state electrons. For this parameter, there is a more dramatic difference resulting from the two sets of wave functions and the relativistic wave functions clearly yield much better agreement with experiment particularly for a fixed scattering angle of 28°. Although the agreement with experiment is not quite as good for 15° scattering, the DWB1CR results are in good qualitative agreement with the shape of the data.

B. Spin-dependent results

Finally we would like to examine spin-dependent cross sections and asymmetries. Spin-up and spin-down cross sections obtained using the nonrelativistic and relativistic wave functions are compared with the experimental data of [19] for $J_f = 1/2$ in Fig. 6 and $J_f = 3/2$ in Fig. 7 for a fixed scattering angle for the faster electron of 28°. A single normalization factor was used for all four sets of data and the factor was chosen to give the best overall agreement between experiment and theory. For the case of $J_f = 1/2$, there is a significant difference between results using nonrelativistic and relativistic wave functions and the relativistic results are consistently closer to experiment. Interestingly for the $J_f = 3/2$ case (and these kinematics), there is essentially no difference between the nonrelativistic and relativistic results. It is important to note, however, that this is not a general rule for $J_f = 3/2$ and that for 15° scattering (not shown), the nonrelativistic and relativistic results were different with the relativistic results being closer to experiment.

In Fig. 8, the spin asymmetries are presented for the two scattering angles for the faster final-state electron and the two J states. Here only the DWB1CR results are shown. Similar to the situation for branching ratios, spin asymmetries are independent of normalization. The agreement between experiment and theory is quite good for 28° and quite bad for 15°. This is particularly interesting in light of the fact that from Fig. 4 we see that the agreement between experiment and theory for spin-averaged cross sections is better for 15° scattering than for 28° scattering. It is clear that the spin-dependent results represent a more sensitive test of theory and for the case of 15° scattering, the present theory would appear to be inadequate. Since the present theory ignores relativistic effects for the projectile electron (e.g., spin-orbit coupling), the logical conclusion would be that this is the source of the problem. However, Mazevet and McCarthy [20] have investigated the importance of including

spin-orbit coupling and they found that it was relatively unimportant.

IV. CONCLUSION

A first-order model for ionization of inert gases by polarized electrons was presented and the results were compared with experiment. It was shown that nonzero spin asymmetries may be obtained using a relatively simple theoretical model in which spin-dependent forces on the spin-polarized projectile are ignored. It was shown that the first-order distorted-wave approximation yields reasonably good agreement with (unnormalized) differential cross sections for both unpolarized and spin-polarized electrons if final-state correlations are included and relativistic wave functions for the atom are used. However, the agreement between experiment and theory is not satisfactory for some kinematics for the spin asymmetry parameter. The logical explanation for this paradox is that a proper theory should include relativistic effects for the projectile electron. However, preliminary calculations by Mazevet and McCarthy [20] indicate that this is not the source of the problem. This is a very new field and we expect that additional theoretical and experimental investigations will help clarify this situation.

ACKNOWLEDGMENTS

D.H.M., V.D.K., and S.J. would like to thank the NSF for financial support, and R.P.M. would like to thank the Natural Sciences and Engineering Research Council of Canada for financial assistance. We would like to thank E. Weigold and his co-workers for permission to use their experimental data prior to publication. We would also like to thank I. McCarthy, S. Mazevet, and F. Hanne for several helpful discussions.

[1] H. Ehrhardt, K. Jung, G. Knoth, and P. Schlemmer, Z. Phys. D **1**, 3 (1986).
[2] G. Baum, W. Blask, P. Freienstein, L. Frost, S. Hesse, W. Raith, P. Rappolt, and M. Streun, Phys. Rev. Lett. **69**, 3037 (1992).
[3] M. Duemmler, G. F. Hanne, and J. Kessler, in *Proceedings of the XVIII International Conference on the Physics of Electronic and Atomic Collisions, Abstracts of Contributed Papers*, edited by T. Andersen, B. Fastrup, F. Folkmann, and H. Knudsen (Aarhus University, Aarhus, Denmark, 1993), p. 144.
[4] G. F. Hanne, Phys. Rep. **95**, 95 (1983).
[5] K. Bartschat and D. H. Madison, J. Phys. B **20**, 5839 (1987).
[6] K. Bartschat and D. H. Madison, J. Phys. B **21**, 2621 (1988).
[7] N. T. Padial, G. D. Menezes, F. J. da Paixao, G. Csanak, and D. C. Cartwright, Phys. Rev. A **23**, 2194 (1990).
[8] G. F. Hanne, in *Correlations and Polarization in Electronic and Atomic Collisions and (e,2e) Reactions*, Institute of Physics Conference Series No. 122, edited by P. J. O. Teubner and E. Weigold (Institute of Physics, Bristol, 1991), p. 15.
[9] N. Anderson, J. W. Gallagher, and I. V. Hertel, Phys. Rep. **165**, 1 (1988).
[10] T. Rösel, J. Röder, L. Frost, K. Jung, H. Ehrhardt, S. Jones, and D. H. Madison, Phys. Rev. A **46**, 2539 (1992).
[11] S. Jones, D. H. Madison, and M. K. Srivastava, J. Phys. B **25**, 1899 (1992).
[12] S. Jones, D. H. Madison, and G. F. Hanne, Phys. Rev. Lett. **72**, 2554 (1994).
[13] D. H. Madison, V. D. Kravtsov, S. Jones, and R. P. McEachran, Can. J. Phys. (to be published).
[14] C. Pan and A. F. Starace, Phys. Rev. A **45**, 4588 (1992).
[15] D. M. Brink and G. R. Satchler, *Angular Momentum* (Oxford University, London, 1968).
[16] H. Ehrhardt, K. H. Hesselbacher, K. Jung, E. Schubert, and K. Willmann, J. Phys. B **7**, 69 (1974).
[17] C. Froese-Fischer, Comput. Phys. Commun. **4**, 107 (1972).
[18] I. P. Grant, B. J. McKenzie, P. H. Norrington, D. F. Mayers, and N. C. Piper, Comput. Phys. Commun. **21**, 207 (1980).
[19] B. Granitza, X. Guo, J. Hurn, Y. Shen, and E. Weigold (unpublished).
[20] S. Mazevet and I. E. McCarthy (private communication).